IJST, Transactions of Civil Engineering, Vol. 38, No. C1+, pp 205-221
Printed in The Islamic Republic of Iran, 2014


# NEURAL NETWORKS FOR DEFLECTIONS IN CONTINUOUS COMPOSITE BEAMS CONSIDERING CONCRETE CRACKING*

S. CHAUDHARY[1**], U. PENDHARKAR[2], K. A. PATEL[3] AND A. K. NAGPAL[4]

[1]Dept. of Civil Engineering, Malaviya National Institute of Technology, Jaipur- 302017, India
Email: schaudhary.ce@mnit.ac.in
[2]School of Engineering and Technology, Vikram University, Ujjain-456010, India
[3, 4]Dept. of Civil Engineering, Indian Institute of Technology Delhi, Hauz Khas, New Delhi-110016, India

**Abstract–** Maximum deflection in a beam is a design criteria and occurs generally at or close to the mid-span. A methodology has been developed for continuous composite beams to predict the inelastic mid-span deflections, $\boldsymbol{d}^{i}$ (considering the cracking of concrete) from the elastic mid-span deflections, $\boldsymbol{d}^{e}$ (neglecting the cracking of concrete). Nine significant structural parameters have been identified that govern the change in mid-span deflections. Six neural networks have been presented to cover the entire practical range of the beams. The proposed neural networks have been validated for a number of beams with different number of spans and the errors are small for practical purposes. The methodology enables rapid estimation of inelastic deflections in continuous composite beams and requires a computational effort that is a fraction of that required for the conventional iterative or incremental analysis. The methodology can easily be extended for large composite building frames where a huge savings in computational effort would result.

**Keywords–** Cracking, composite beam, deflection, neural networks, sensitivity analysis

## 1. INTRODUCTION

Steel-concrete composite beams (Fig. 1a) are an integral part of steel-concrete composite bridges and composite frames. There may be cracking of concrete slab of continuous composite beams near interior supports where moments are high. This may result in moment redistribution and considerable change in deflections of the beam. The appropriate prediction of mid-span deflections after moment redistribution owing to the cracking of concrete is important from serviceability considerations. Methods are available in the literature for the same [1]. These methods are based either on incremental or iterative approach. Both approaches require a computational effort, which is many times more than that required for the elastic analysis (neglecting cracking). The computational effort required may be huge for large composite structures. The use of neural network may be made to drastically reduce the computational effort in such cases.

Neural networks have been extensively applied in the various field of civil engineering. Some of the applications of neural networks in the field of civil/structural engineering include development of performance evaluation systems for concrete bridges [2,3], prediction of time effects in reinforced concrete frames [4], estimation of concrete strength [5, 6], prediction of web crippling strength of cold-formed steel sheetings [7], bending moment prediction for continuous composite beams considering concrete cracking [8], estimation of ultimate pure bending of steel circular tubes [9], determination of shear strength in circular reinforced concrete columns [10], prediction of torsional strength of reinforced

*Received by the editors April 2, 2013; Accepted October 26, 2013.
**Corresponding author

concrete beams [11], investigatation the effect of natural and steel fibers on the performance of concrete [12], response prediction of offshore floating structure [13], prediction of the performance of two rotating biological contactor systems in removal of hydroquinone [14], forecasting of ground water depth [15], prediction of response spectrum based spatially varying earthquake [16] and identification of most probable pollution source in rivers of Iran [17]. Recently, the feed forward back propagation neural network and adaptive network based fuzzy inference system (ANFIS) [18, 19] have been modeled to predict the deflection of high strength self compacting concrete (HSSCC) deep beams using experimental data.

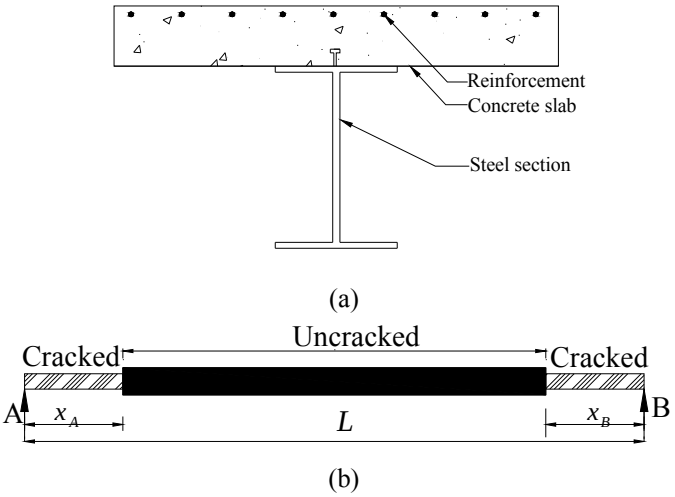


Fig. 1. (a) Composite cross-section and (b) cracked span length beam element

In this paper, a methodology using neural networks has been developed for continuous composite beams to predict the inelastic mid-span deflections, $d^i$ (considering the cracking of concrete) from the elastic mid-span deflections, $d^e$ (neglecting the cracking of concrete). The elastic deflections can be obtained from any of the readily available softwares. The methodology enables rapid estimation of inelastic deflections and requires a computational effort that is a fraction of that required for the methods available in the literature. The proposed neural networks have been validated for a number of example beams. The errors are shown to be small for practical purposes. The methodology can easily be extended for large composite building frames where a very huge saving in computational effort would result.

## 2. ITERATIVE METHOD OF ANALYSIS

For generalized and efficient neural networks, a large number of training data sets are required for which a highly efficient method is desirable. A hybrid analytical-numerical procedure has been developed to take into account the nonlinear effects of concrete cracking near interior supports and time-dependent effects of creep and shrinkage in composite beams and frames [20, 21]. The procedure is analytical at the element level and numerical at the structural level. A cracked span length beam element, consisting of two cracked zones of length $x_A$ and $x_B$ at the ends A and B respectively, and an uncracked zone in the middle (Fig. 1b) has therefore been used in the procedure [20, 21]. For a completely cracked beam element of total length $L$, $x_A$ and $x_B$ would be equal to $L/2$ and for a completely uncracked beam element $x_A$ and $x_B$ would be equal to zero. The closed form expressions for crack lengths, flexibility matrix coefficients, end displacements and mid-span deflection of the cracked span length beam element are used in the procedure [20, 21]. Tension stiffening effect is taken into account by evaluating interpolation coefficients according to CEB-FIP 1993 [22].

The analysis considering concrete cracking is carried out using an iterative method. Consider a typical iterative cycle. A displacement analysis is carried out in the beginning of the cycle for the residual force vector of the continuous composite beam at the end of the previous cycle. Revised force vector and displacement vector are obtained by adding the force vector and displacement vector obtained from this analysis to the force vector and displacement vector at the end of the previous cycle. Crack lengths and interpolation coefficients are then updated according to the revised force vector.

Changes in the cracking state of the sections (cracked or uncracked) and thereby in the end rotations of the beam elements lead to the difference between the displacement vector of these elements obtained from the displacement analysis and that obtained by the principle of virtual work involving integration of curvature diagram of a member. The residual force vector corresponding to this error in displacement vector can be obtained using the revised stiffness matrix of the beam element.

Residual force vector of the continuous composite beam (obtained by assembling the residual force vector of the beam elements) should be within permissible limit [1] for the iterative process to terminate; otherwise a new cycle is started. Required deflections are obtained after convergence is achieved.

The procedure has been validated by comparison with the experimental results, analytical results, and finite element model.

## 3. SIGNIFICANT EXTENT OF PROPAGATION OF THE EFFECT OF CRACKING

The change in mid-span deflection of a span due to cracking at a support varies with the position of the span with respect to the cracked support. The further the span from the support, the smaller the change. A preliminary numerical study is therefore carried out to estimate the significant extent of propagation of the effect of cracking at a support.

For the study, a typical multi-span (number of span $=n$) continuous composite beam is considered (Fig. 2a). The cross-sectional properties throughout the beam are kept constant, as is generally the practice. The nature of the elastic deflection diagram for the beam with equal spans ($l = l_1 = l_2 = l_3 ..... = l_n$, the subscripts here and subsequently in other quantities indicate either the span number or the support number) and the same load intensities ($w = w_1 = w_2 = ... = w_j .... = w_n$) are shown in Fig. 2b.

Let $\eta \left[ = 100 \times \delta d / l \right]$, the variation in elastic mid-span deflection $\left( \delta d = d^i - d^e \right)$ normalized with respect to $l$, be a measure of the extent of propagation of the effect of cracking at a support. A smaller value of $\eta$ would indicate that the effect of cracking on mid-span deflection is minimal and vice versa.

In practical cases, though the cross-sectional properties are the same throughout the beam, one of the spans (exterior span or next to exterior span or interior span) may be heavily loaded or may be larger than other spans leading to large moments at its supports and thereby to cracking. Two cases are considered here in detail to identify the significant extent of propagation of the effect of cracking. In case 1, it is assumed that an exterior span (1st span) is loaded heavily thereby leading to cracking at penultimate support (support 2). In case 2, it is assumed that an interior span (say 5th span) is loaded heavily thereby leading to cracking at its supports (supports 5 and 6). For both cases, a beam with $n$=10, $l_j$ ($j = 1$ to $n$)=8.0 m and $M^{cr} = 25.12$ kN-m is considered and initially the loading on the spans is kept equal to the cracking load, $w^{cr}$ (the load at which the moment at any section of the beam just becomes equal to $M^{cr}$).

Consider case 1. The load on 1st span is increased (Fig. 2c), keeping the loads on other spans constant, such that the cracking takes place only in the 1st and 2nd spans at support 2 resulting in the change in mid-span deflections of the beam (Fig. 2d). This change varies with the ratio $M^{cr} / M_2^e$ (designated as the cracking moment ratio at support 2). Nine values ($1.0, 0.90, 0.8, 0.7, 0.60, 0.50, 0.40, 0.30, 0.25$) of $M^{cr} / M_2^e$ resulting from the increase in $w_1$ are

considered. The magnitude of $\eta$ for the cracked spans ( 1st and 2nd spans), first span next to the right cracked span (2nd span), i.e. 3rd span, second span next to the right cracked span, i.e. 4th span are shown in Fig. 3. Only the variations $\eta_1$, $\eta_2$, $\eta_3$ may be considered to be significant.

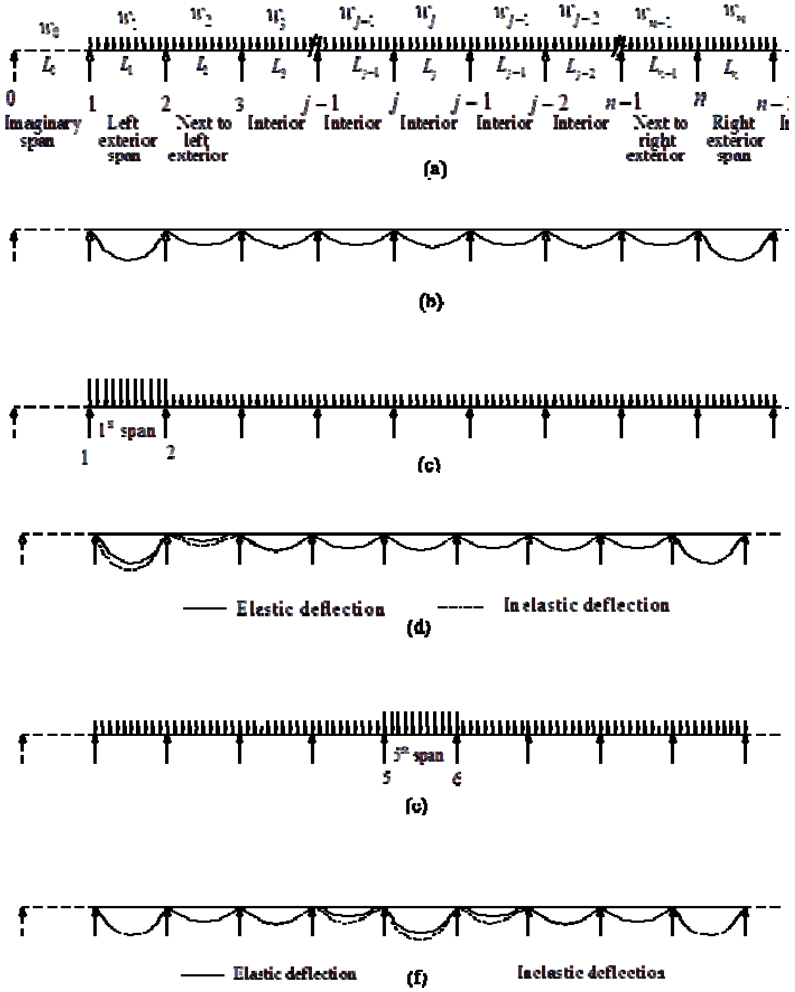


Fig. 2. A typical multi-span continuous composite beam, (a) geometry and loading, (b) elastic deflection diagram (equal spans and equal loadings), (c) 1st span loaded heavily, (d) elastic and inelastic deflection diagrams (1st span loaded heavily), (e) 5th span loaded heavily and (f) elastic and inelastic deflection diagrams (5th span loaded heavily)

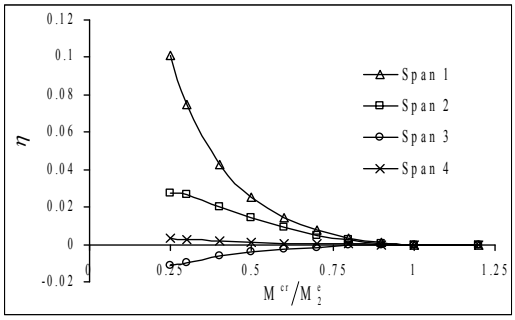


Fig. 3. Variation of $\eta$ for different spans with $M^{cr}/M_2^e$ for cracking at support 2

Now consider case 2 in which cracking occurs only in the 4th, 5th and 6th spans at two adjacent intermediate supports (supports 5 and 6). For this purpose, $w_5$ is increased (Fig. 2e) and again nine values of $M^{cr}/M_5^e$ (and $M^{cr}/M_6^e$) are considered. The natures of elastic and inelastic deflection diagrams for this case are shown in Fig. 2f. The magnitude of $\eta$ for the cracked spans (4th, 5th and 6th spans), first

spans next to the cracked spans (4th and 6th spans), i.e. 3rd and 7th spans, second spans next to the cracked spans, i.e. 2nd and 8th spans are shown in Fig. 4. Only $\eta_3$ , $\eta_4$ , $\eta_5$ , $\eta_6$ , $\eta_7$ may be considered to be significant.

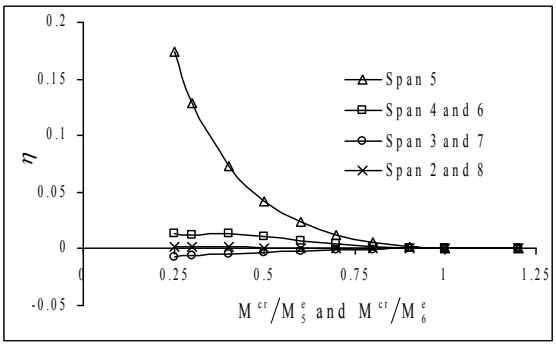


Fig. 4. Variation of $\eta$ for different spans with $M^{cr}/M_5^e$ (and $M^{cr}/M_6^e$ ) for cracking at adjacent interior supports (Supports 5 and 6)

Therefore, it is observed from both cases that the change in mid-span deflections may be considered to be significant only for the cracked spans and first spans next to the cracked spans.

Similar numerical studies are carried out for beams with different $l_j$, $n$ and $M^{cr}$. From these studies also (not reported here), similar observations are made.

It therefore follows that in order to establish change in the mid-span deflection of $j^{th}$ span with sufficient accuracy, only cracking at the supports (supports $j$ and $j+1$) of the span and adjacent supports (supports $j-1$ and $j+2$) needs to be considered.

## 4. PROBABLE STRUCTURAL PARAMETERS AND SENSITIVITY ANALYSIS

Let the change in mid-span deflection for a span of a beam may be expressed in the form of a non-dimensional parameter $\delta d/d^{eq}$, where $d^{eq}$ = mid-span deflection of an equivalent fixed beam (uncracked fixed beam with the same $l$ and $w$ as those of the span). A sensitivity analysis is carried out to determine the significant structural parameters governing $\delta d_j/d_j^{eq}$ for $j^{th}$ span. The significant structural parameters would be the input parameters and $\delta d_j/d_j^{eq}$ would be the output parameter for the neural networks.

For the sensitivity analysis, two span ($n$=2), three span ($n$=3) and nine span ($n$=9) beams are considered. Further, nine span beam may represent all the beams having spans greater than three. Therefore, these sets of beams may be considered to represent continuous composite beams with any number of spans.

It has been observed in the previous section that the change in mid-span deflection of $j^{th}$ span is significantly affected by cracking at its supports (supports $j$ and $j+1$) and adjacent supports (supports $j-1$ and $j+2$) only. Accordingly, the probable structural parameters, which may influence $\delta d_j/d_j^{eq}$ with the same cross-section throughout the length of the beam (Fig. 2a), are listed below:

1. Inertia ratio, $I^{cr}/I^{un}$, where $I^{un}$ = transformed moment of inertia of uncracked composite section and $I^{cr}$ = transformed moment of inertia of cracked section consisting of steel section and reinforcement only.
2. Stiffness ratio, $S_{j-1}/S_j$ ( $S_j = E_c I^{un}/l_j$, where $E_c$ = modulus of elasticity of concrete ), of adjacent spans at left support of the span.
3. Stiffness ratio ( $S_{j+1}/S_j$ ) of adjacent spans at right support of the span.
4. Load ratio ( $w_{j-1}/w_j$ ) of adjacent spans at left support of the span.
5. Load ratio ( $w_{j+1}/w_j$ ) of adjacent spans at right adjacent support of the span.

6. Cracking moment ratio ( $M^{cr}/M^{e}_{j-1}$ ) at left support of the left span.
7. Cracking moment ratio ( $M^{cr}/M^{e}_{j}$ ) at left support of the span.
8. Cracking moment ratio ( $M^{cr}/M^{e}_{j+1}$ ) at right support of the span.
9. Cracking moment ratio ( $M^{cr}/M^{e}_{j+2}$ ) at right support of the right adjacent span.

The practical range for $I^{cr}/I^{un}$ may be considered as 0.37-0.57 and for the other eight probable structural parameters as 0.25-4.0 [8]. Sensitivity studies are carried out for the left exterior span (1st span) of two span, three span and nine span beams and for a typical interior span (5th span) of a nine span beam. In these studies, only one parameter is varied at a time, keeping the other parameters constant [ average value of the practical range for first five probable structural parameters and average value (0.625) of the range (0.25-1), which involves cracking, for $M^{cr}/M^{e}_{j-1}$, $M^{cr}/M^{e}_{j}$, $M^{cr}/M^{e}_{j+1}$, $M^{cr}/M^{e}_{j+2}$ ]. It may be noted that since the cross-sections of the beams are the same throughout the length, the required stiffness ratios $S_{j-1}/S_j$ or $S_{j+1}/S_j$ for the studies are achieved by varying the lengths of spans. The lengths $l_j\,(j=1 \text{ to } n)$ are initially taken as 8.0 m unless otherwise stated.

### *a) Left exterior span*

Sensitivity analysis is carried out for left exterior span $(j=1)$ and significant structural parameters are identified. For this span an imaginary span (Fig. 2a) needs to be considered for which $w_0$ and $l_0$ are assumed to be very small. The variation of output parameter $\delta d_1/d_1^{eq}$ with the probable structural parameters is studied. It may be noted that out of the nine probable structural parameters, the ratios $S_0/S_1$, $w_0/w_1$, $M^{cr}/M^{e}_{0}$ and $M^{cr}/M^{e}_{1}$ need not be considered as $S_0/S_1$, $w_0/w_1$, $M^{cr}/M^{e}_{0}$ involve the imaginary span and moment at support 1 is always equal to zero. Additionally, cracking moment ratio $M^{cr}/M^{e}_{3}$ also need not be considered for two span beam, as the moment at support 3 is always equal to zero.

**(1) *Effect of inertia ratio*** $\left(I^{cr}/I^{un}\right)$ : The stiffness of an uncracked composite section, $I^{un}$, reduces to that of steel section and reinforcement only, $I^{cr}$ on cracking, which leads to change in mid-span deflections. Therefore, $I^{cr}/I^{un}$ is considered as a probable structural parameter. The other structural parameters have been kept constant ( $S_2/S_1=1.00$, $w_2/w_1=1.00$, $M^{cr}/M^{e}_{2}=0.625$ for two span beam and $S_2/S_1=1.00$, $w_2/w_1=1.00$, $M^{cr}/M^{e}_{2}=0.625$, $M^{cr}/M^{e}_{3}=0.625$ for three and nine span beams). The variations are shown in Fig. 5 and these are significant and almost linear for all three beams. As expected, the redistribution is more for the lower values of $I^{cr}/I^{un}$. Further, these variations can be represented fairly accurately by considering two values (0.37, 0.57) designated as sampling points of $I^{cr}/I^{un}$.

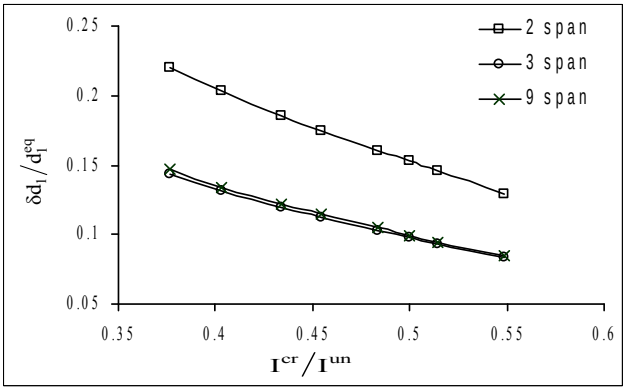


Fig. 5. Variation of $\delta d_1/d_1^{eq}$ with $I^{cr}/I^{un}$ for 2, 3 and 9 span beams

**(2) *Effect of stiffness ratio*** $\left(S_2/S_1\right)$ ***at right support:*** The change in mid-span deflection of a span due to cracking of concrete may vary with the relative stiffness of the span and adjacent spans; hence stiffness ratio $S_2/S_1$ has been considered as a probable structural parameter. The other structural parameters have been kept constant ($I^{cr}/I^{un}=0.4547$, $w_2/w_1=1.00$, $M^{cr}/M_2^e=0.625$ for 2 span beam and $I^{cr}/I^{un}=0.4547$, $w_2/w_1=1.00$, $M^{cr}/M_2^e=0.625$, $M^{cr}/M_3^e=0.625$ for 3 and 9 span beams). The ratio $S_2/S_1$ has been varied by varying the length of $2^{nd}$ span. The variations have been plotted with $\log\left(S_2/S_1\right)$ for fair representation of the ratio $S_2/S_1$ in both cases: (i) when it is smaller than one and (ii) when it is greater than one. The variations are shown in Fig. 6 and are significant for all the beams. The dotted portions in the figure denote small elastic deflection. Those deflections, which are less than half of the mid-span deflection of the fixed beam with the same properties as those of the span and subjected to $w^{cr}$, have been assumed to be small and have been neglected in the present study since these deflections are not important from the design point of view. The variations for all the beams (two span, three span and nine span beams) can be represented fairly accurately by considering five sampling points (log ($S_2/S_1$) = $-0.602, -0.301, 0.0, 0.301, 0.602$).

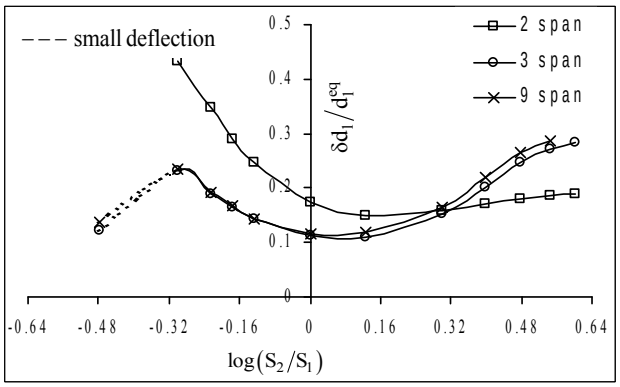


Fig. 6. Variation of $\delta d_1/d_1^{eq}$ with $S_2/S_1$ for 2, 3 and 9 span beams

**(3) *Effect of load ratio*** $\left(w_2/w_1\right)$ ***at right support:*** Ratio of loading on the span and adjacent spans may affect the change in mid-span deflection, therefore, $w_2/w_1$ is also considered as a probable structural parameter. The other structural parameters have been kept constant ($I^{cr}/I^{un}=0.4547$, $S_2/S_1=1.00$, $M^{cr}/M_2^e=0.625$ for two span beam and $I^{cr}/I^{un}=0.4547$, $S_2/S_1=1.00$, $M^{cr}/M_2^e=0.625$, $M^{cr}/M_3^e=0.625$ for three and nine span beams). The variations are shown in Fig. 7 and are significant for all the beams. Again, the variations for all the beams (two span, three span and nine span beams) can be represented fairly accurately by considering four sampling points (log ($w_2/w_1$) = $-0.602, 0.0, 0.301, 0.602$).

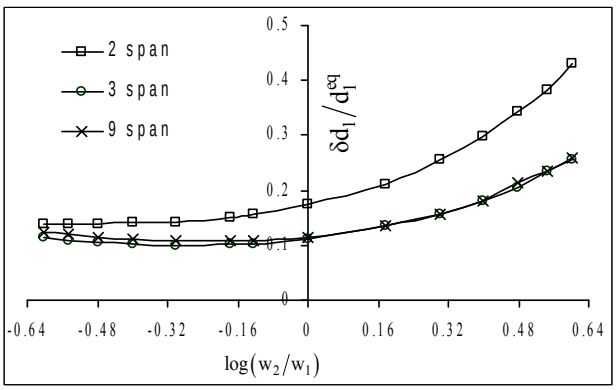


Fig. 7. Variation of $\delta d_1/d_1^{eq}$ with $w_2/w_1$ for 2, 3 and 9 span beams

**(4) *Effect of cracking moment ratio* $\left(M^{cr}/M_2^e\right)$ *at right support:*** Since the change in mid-span deflection of a span varies with ratio $M^{cr}/M^e$ at the supports of the span (Figs. 3 and 4), $M^{cr}/M_2^e$ is selected as a probable structural parameter. The other structural parameters have been kept constant as $I^{cr}/I^{un}=0.4547$, $S_2/S_1=1.00$, $w_2/w_1=1.00$ for two span beam and $I^{cr}/I^{un}=0.4547$, $S_2/S_1=1.00$, $w_2/w_1=1.00$, $M^{cr}/M_3^e=0.625$ for three span and nine span beams. The variations are shown in Fig. 8 and are significant for all three beams. There is no variation in case of two span beam for $M^{cr}/M_2^e$ greater than 1 as there is no cracking. Further, though the variations for all the beams are different, these can, however, be represented fairly accurately by considering three sampling points (log ($M^{cr}/M_2^e$) $=-0.602, 0.0, 0.602$).

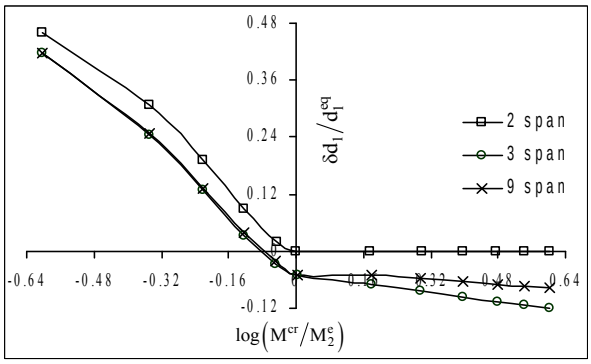


Fig. 8. Variation of $\delta d_1/d_1^{eq}$ with $M^{cr}/M_2^e$ for 2, 3 and 9 span beams

**(5) *Effect of cracking moment ratio*** $\left(M^{cr}/M_3^e\right)$ ***at right adjacent support:*** The change in mid-span deflection of a span depends on cracking at the adjacent supports also (Figs. 3 and 4), therefore $M^{cr}/M_3^e$ is selected as a probable structural parameter for three and nine span beams. The other structural parameters have been kept constant ($I^{cr}/I^{un}=0.4547$, $S_2/S_1=1.00$, $w_2/w_1=1.00$, $M^{cr}/M_2^e=0.625$). The variations are shown in Fig. 9. The variations for both beams are significant and tend to assume a constant value for $M^{cr}/M_3^e$ greater than 1. Again, though the variations for three span and nine span beams are different, these can be represented fairly accurately by considering three sampling points (log ($M^{cr}/M_3^e$) = $-0.602, 0.0, 0.602$).

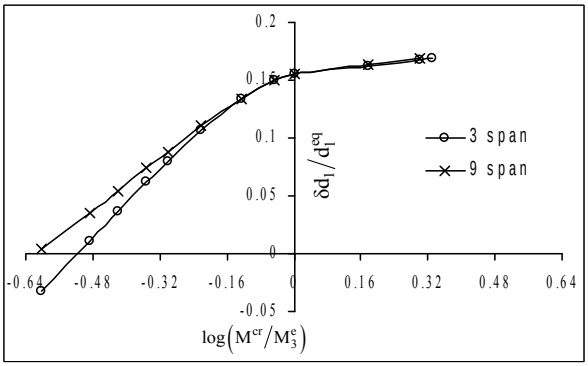


Fig. 9. Variation of $\delta d_1/d_1^{eq}$ with $M^{cr}/M_3^e$ for 2, 3 and 9 span beams

Similar studies for the above probable structural parameters ($I^{cr}/I^{un}$, $S_2/S_1$, $w_2/w_1$, $M^{cr}/M_2^e$ for two span beam and $I^{cr}/I^{un}$, $S_2/S_1$, $w_2/w_1$, $M^{cr}/M_2^e$, $M^{cr}/M_3^e$ for three span and nine span beams) are carried out for $l_j(j=1, 3 \text{ to } n)$ = 4.0 m and 12.0 m also. The same variations as shown in Figs. 5-9 are obtained. Therefore the absolute span length is not a parameter which governs the output parameter $\delta d/d^{eq}$ for an exterior span.

Further, the nature of the variations for the right exterior span of the beams, i.e. $n^{th}$ span for $n$ span beams ( $n$ =2, 3, 9) would be similar to that observed for the 1st span of the beams.

***b) Interior span***

Similar studies as performed for the sensitivity analysis of 1st span are carried out for the sensitivity analysis of a typical interior span (5th span, $j=5$) of nine span beam (there are no interior spans for two span and three span beams). There are again nine probable structural parameters [ $I^{cr}/I^{un}$ , $S_4/S_5$ , $S_6/S_5$ , $w_4/w_5$ , $w_6/w_5$ , $M^{cr}/M_4^e$ , $M^{cr}/M_5^e$ , $M^{cr}/M_6^e$ , $M^{cr}/M_7^e$ ] and one output parameter [ $\delta d_5/d_5^{eq}$ ]. It may be noted that since it is difficult to keep eight other parameters constant while carrying out sensitivity analysis for one parameter, keeping in view the symmetry of the beams, parameters have been varied in pairs. The pairs chosen are $S_4/S_5$ , $S_6/S_5$ ; $w_4/w_5$ , $w_6/w_5$ ; $M^{cr}/M_4^e$ , $M^{cr}/M_7^e$ ; and $M^{cr}/M_5^e$ , $M^{cr}/M_6^e$ . The variations are shown in Figs. 10-14, where dotted portions denote very small deflections as explained earlier. The variations are seen to be similar to corresponding variations for exterior spans, therefore the same sampling points as for exterior spans may also be chosen for interior span

Again, similar studies are carried out for span lengths $l_j$ ($j$ =1 to 3, 5 and 7 to 9) = 4.0 m and 12.0 m and the same results are obtained irrespective of the absolute span lengths, as has been observed earlier for the exterior span.

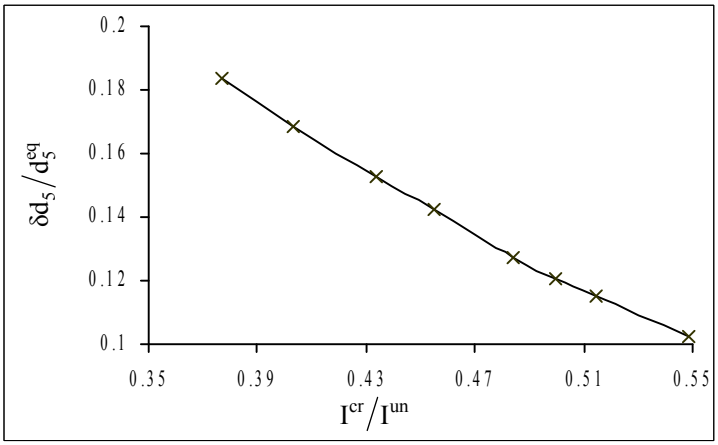


Fig. 10. Variation of $\delta d_5/d_5^{eq}$ with $I^{cr}/I^{un}$ for 9 span beam

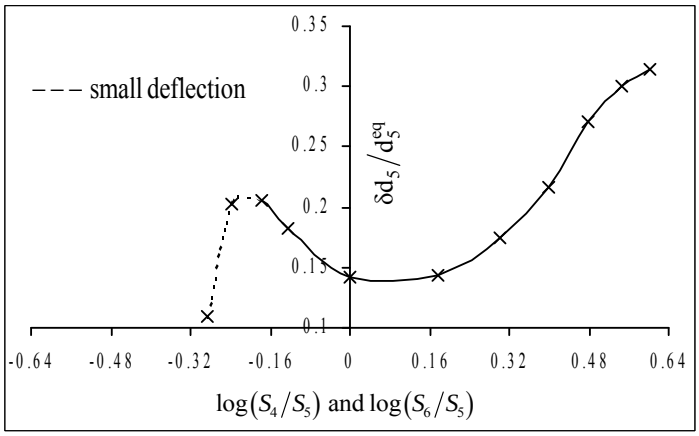


Fig. 11. Variation of $\delta d_5/d_5^{eq}$ with $S_4/S_5$ and $S_6/S_5$ for 9 span beam

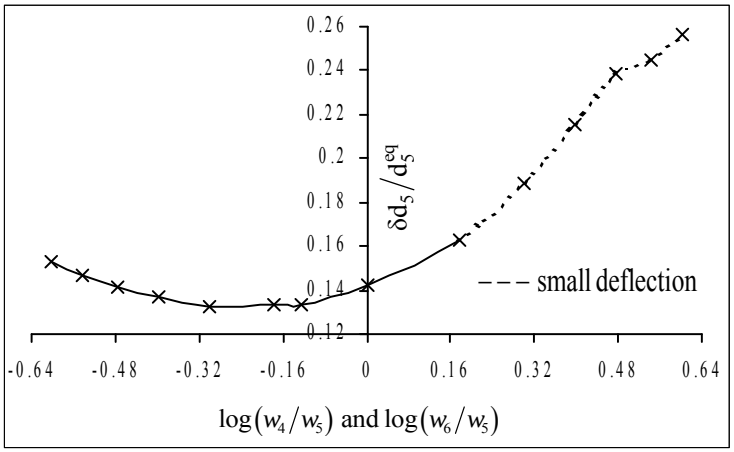


Fig. 12. Variation of $\delta d_5/d_5^{eq}$ with $w_4/w_5$ and $w_6/w_5$ for 9 span beam

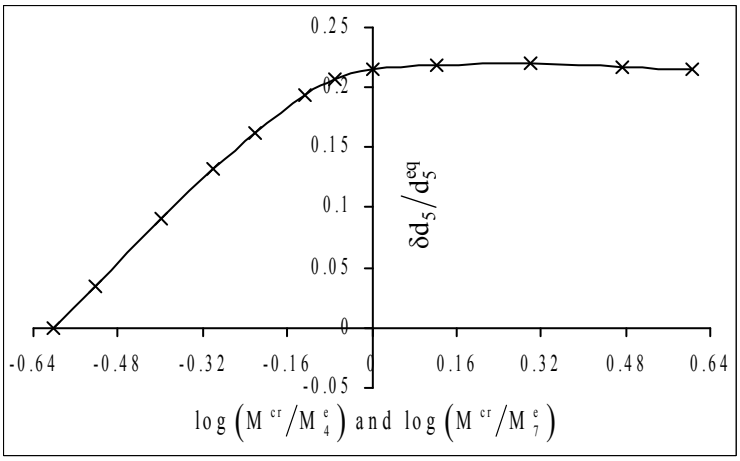


Fig. 13. Variation of $\delta d_5/d_5^{eq}$ with $M^{cr}/M_4^e$ and $M^{cr}/M_7^e$ for 9 span beam

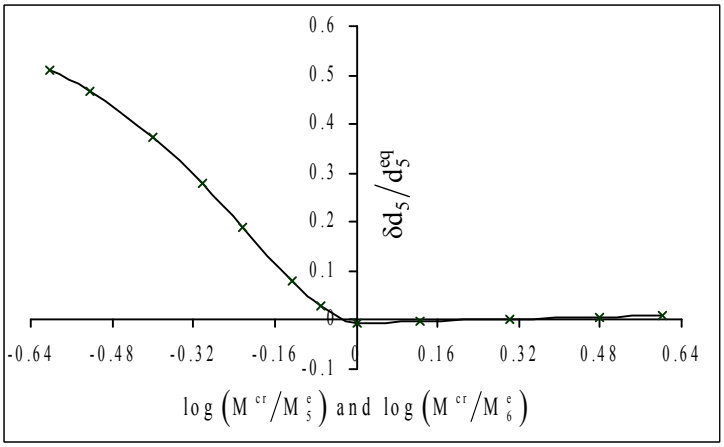


Fig. 14. Variation of $M_5^i/M_5^e$ with $M^{cr}/M_5^e$ and $M^{cr}/M_6^e$ for 9 span beam

## 5. NEURAL NETWORKS AND SAMPLING POINTS

It is observed from the sensitivity analysis that all nine probable structural parameters $I^{cr}/I^{un}$, $\log\left(S_{j-1}/S_j\right)$, $\log\left(S_{j+1}/S_j\right)$, $\log\left(w_{j-1}/w_j\right)$, $\log\left(w_{j+1}/w_j\right)$, $\log\left(M^{cr}/M^{e}_{j-1}\right)$, $\log\left(M^{cr}/M^{e}_{j}\right)$, $\log\left(M^{cr}/M^{e}_{j+1}\right)$, $\log\left(M^{cr}/M^{e}_{j+2}\right)$ are significant. It is also observed that the magnitude of variations for two span, three span and nine span beams are different. Therefore two span, three span and nine span beams are considered separately for developing the neural networks. As has been stated earlier, nine span beam may represent all the beams having spans greater than three.

Further, for each type of beam, separate neural networks have been developed for exterior spans, next to exterior spans and interior spans keeping in mind the involvement of imaginary spans and exterior supports for exterior spans and next to exterior spans**.** For two span beams, one network has been developed for exterior spans (NN1); for three span beams, two networks have been developed one each for exterior spans (NN2) and next to exterior spans (NN3), whereas for nine span beams three networks have been developed one each for exterior spans (NN4), next to exterior spans (NN5) and interior spans (NN6).

The neural networks chosen in the present study are multilayered feed-forward networks with neurons in all the layers fully connected in feed forward manner (Fig. 15). Sigmoid function is used as an activation function and the back propagation learning algorithm is used for training. The back propagation algorithm has been used successfully for many structural engineering applications [4,5,8,10,12,14,16,18] and is considered as one of the efficient algorithms in engineering applications [23]. One hidden layer is chosen and the number of neurons in the layer is decided in the learning process by trial and error.

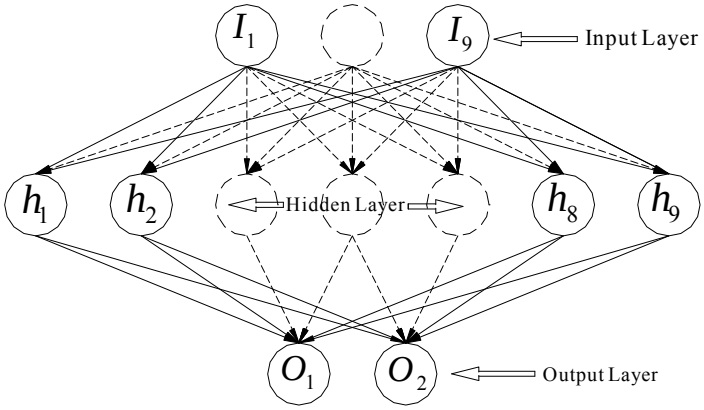


Fig. 15. Configuration of a typical neural network

As stated earlier, the input consists of significant structural parameters, which now have been identified as $I^{cr}/I^{un}$, $\log\left(S_{j-1}/S_j\right)$, $\log\left(S_{j+1}/S_j\right)$, $\log\left(w_{j-1}/w_j\right)$, $\log\left(w_{j+1}/w_j\right)$, $\log\left(M^{cr}/M^{e}_{j-1}\right)$, $\log\left(M^{cr}/M^{e}_{j}\right)$, $\log\left(M^{cr}/M^{e}_{j+1}\right)$, $\log\left(M^{cr}/M^{e}_{j+2}\right)$, whereas the output consists of $\delta d_j/d^{eq}_j$. It has been noted earlier from Figs. 5-14 that the significant structural parameters and sampling points for the interior spans are the same as those for the exterior spans, therefore, the same significant structural parameters (input parameters) and sampling points may be assumed for next to exterior spans also.

The sampling points for the input parameters are summarized in Table 1. It may be noted that wherever imaginary spans are involved, high values (10) of stiffness ratios are assumed for $S_{j-1}/S_j$ and $S_{j+1}/S_j$. Therefore, a value of 1.0 has been indicated in the Table 1 for $\log\left(S_{j-1}/S_j\right)$ and $\log\left(S_{j+1}/S_j\right)$ in such cases. Similarly, the values of cracking moment ratios $M^{cr}/M^{e}_{j-1}$, $M^{cr}/M^{e}_{j}$, $M^{cr}/M^{e}_{j+1}$ and

$M^{cr}/M^{e}_{j+2}$ are also assumed to be high (10) at exterior supports and imaginary supports and therefore, again, a value of 1.0 has been considered for log of these cracking moment ratios. On the other hand, the value of load ratios $w_{j-1}/w_j$ and $w_{j+1}/w_j$ are assumed to be very small (0.1) wherever imaginary spans are involved and therefore a value of -1.0 has been considered for $\log\left(w_{j-1}/w_j\right)$ and $\log\left(w_{j+1}/w_j\right)$ in such cases.

## 6. TRAINING OF NEURAL NETWORK

Since the training of a neural network is an essential step in its performance, a sufficiently large database should be generated for the training, validating and testing. The performance of a neural network depends significantly on the numbers of training, validating and testing data and the domain this data covers**.**

For each network, different combinations of sampling points of the input parameters and the resulting values of the output parameter are considered. Each such combination of the input parameters and the output parameter comprises a data set. Some of the combinations of input parameters are impractical, therefore such combinations have been ignored. Instead, additional combinations of the parameters have been considered wherever possible. It may be noted that the data sets for which $d^e$ are small (defined earlier) have been neglected. It may be noted that for two span beams (NN1 network), two additional sampling points (-0.301, -0.125) for $\log\left(M^{cr}/M^{e}_{2}\right)$ were required to obtain good test results. The total number of data sets used for training, validating and testing of the networks NN1 to NN6 are 240, 476, 54, 476, 4460, 59680 respectively.

Table 1. Sampling points for input parameters

| Beam | Span | Input Parameters | | | | | | | | |
|---|---|---|---|---|---|---|---|---|---|---|
| | | $I^{cr}/I_{un}$ | $\frac{b}{(L_i+L_{i+1})}$ | $\frac{b}{(L_i+L_{i+1})}$ | $\frac{w_{i-1}}{w_i}$ | $\frac{w_{i+1}}{w_i}$ | $\frac{M^{cr}}{M^{e}_{i-1}}$ | $\frac{M^{cr}}{M^{e}_{i}}$ | $\frac{M^{cr}}{M^{e}_{i+1}}$ | $\frac{M^{cr}}{M^{e}_{i+2}}$ |
| 2 span | Left exterior | 0.37, 0.57 | 1.00 | -0.602,-0.302,0,0.301,0.602 | -1.00 | -0.602,0,0.301,0.602 | 1.00 | 1.00 | -0.602,0,0.602 | 1.00 |
| | Right exterior | 0.37, 0.57 | -0.602,-0.301,0,0.301,0.602 | 1.00 | -0.602,0,0.301,0.602 | -1.00 | 1.00 | -0.602,0,0.602 | 1.00 | 1.00 |
| 3 span | Left exterior | 0.37, 0.57 | 1.00 | -0.602,-0.301,0,0.301,0.602 | -1.00 | -0.602,0,0.301,0.602 | 1.00 | 1.00 | -0.602,0,0.602 | -0.602,0,0.602 |
| | Right exterior | 0.37, 0.57 | -0.602,-0.301,0,0.301,0.602 | 1.00 | -0.602,0,0.301,0.602 | -1.00 | -0.602,0,0.602 | -0.602,0,0.602 | 1.00 | 1.00 |
| | Next to exterior | 0.37, 0.57 | -0.602,-0.301,0,0.301,0.602 | -0.602,-0.301,0,0.301,0.602 | -0.602,0,0.301,0.602 | -0.602,0,0.301,0.602 | 1.00 | -0.602,0,0.602 | -0.602,0,0.602 | 1.00 |
| 9 span | Left exterior | 0.37, 0.57 | 1.00 | -0.602,-0.301,0,0.301,0.602 | -1.00 | -0.602,0,0.301,0.602 | 1.00 | 1.00 | -0.602,0,0.602 | -0.602,0,0.602 |
| | Right exterior | 0.37, 0.57 | -0.602,-0.301,0,0.301,0.602 | 1.00 | -0.602,0,0.301,0.602 | -1.00 | -0.602,0,0.602 | -0.602,0,0.602 | 1.00 | 1.00 |
| | Next to left exterior | 0.37, 0.57 | -0.602,-0.301,0,0.301,0.602 | -0.602,-0.301,0,0.301,0.602 | -0.602,0,0.301,0.602 | -0.602,0,0.301,0.602 | 1.00 | -0.602,0,0.602 | -0.602,0,0.602 | -0.602,0,0.602 |
| | Next to right exterior | 0.37, 0.57 | -0.602,-0.301,0.,0.301,0.602 | -0.602,-0.301,0,0.301,0.602 | -0.602,0,0.301,0.602 | -0.602,0,0.301,0.602 | -0.602,0,0.602 | -0.602,0,0.602 | -0.602,0,0.602 | 1.00 |
| | Interior | 0.37, 0.57 | -0.602,-0.301,0,0.301,0.602 | -0.602,-0.301,0,0.301,0.602 | -0.602,0,0.301,0.602 | -0.602,0,0.301,0.602 | -0.602,0,0.602 | -0.602,0,0.602 | -0.602,0,0.602 | -0.602,0,0.602 |

It may be further noted that both the left and the right exterior spans have been considered for the training of exterior spans of two span, three span and nine span beams and similarly both next to left exterior spans as well as next to right exterior spans, have been considered for training of next to exterior spans of 9 span beams. This makes the application of neural network simpler.

In order to bring the output parameters in the range –1.0 to 1.0, biases are added to the output parameters before normalization. The biases and normalization are shown in Table 2.

Table 2. Details of neural networks

| S. No. | Network | Bias | Normalization factor | Configuration | MSE |
|---|---|---|---|---|---|
| 1 | NN1 | 0.000 | 1.00 | 09-15-01 | 0.00003 |
| 2 | NN2 | 0.681 | 1.75 | 09-18-01 | 0.00003 |
| 3 | NN3 | 0.000 | 1.00 | 09-09-01 | 0.00004 |
| 4 | NN4 | 0.850 | 2.00 | 09-18-01 | 0.00002 |
| 5 | NN5 | 1.200 | 2.50 | 09-23-01 | 0.00006 |
| 6 | NN6 | 0.300 | 1.20 | 09-17-01 | 0.00012 |

The training is carried out using the Stuttgart Neural Network Simulator [24]. For each network, 70% of the data sets are used for the training (as training patterns) whereas 15% of the data sets are used for the validating and the testing each. For this partitioning, 'hold out method' [25], in which partitioning is done randomly, has been adopted. To train the neural network, back-propagation algorithm updates the weight and bias values to achieve a desired input-output relationship in each iteration that generates output values that are closer to the target values. For training, several trials are carried out with different numbers of neurons in the hidden layer. Care is taken that the mean square error for test results does not increase with the number of neurons in hidden layer or epochs (overtraining). The configurations (number of input parameters-number of neurons in hidden layer- number of output parameters) of all the six networks which yield the least mean square errors (MSE) and the corresponding mean square errors of training are also shown in Table 2.

## 7. VALIDATION OF NEURAL NETWORKS

Trained neural networks are validated for a number of beams with a wide variation of input parameters. Six example beams (EB1-EB6) are considered (Fig. 16). The value of $I^{cr}/I^{un}$ for these beams is 0.4243, 0.5144, 0.4243, 0.4547, 0.4243, and 0.4547 respectively.

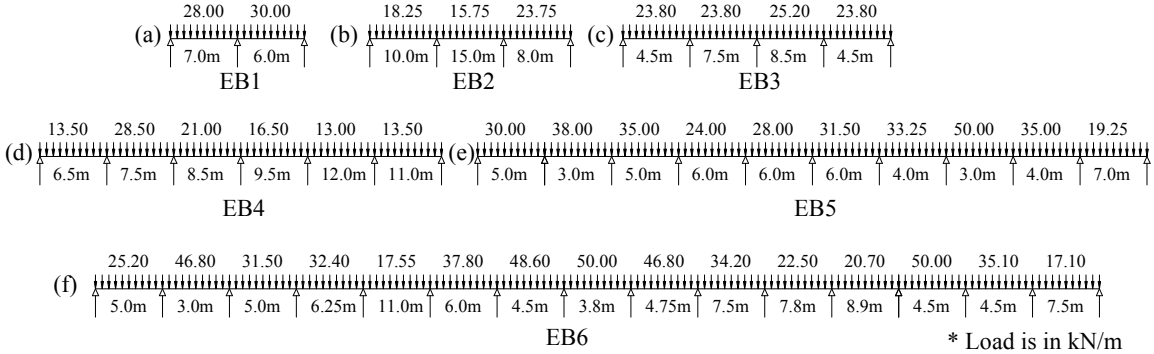


Fig. 16. Example beams (a) two span beam (EB1), (b) three span beam (EB2), (c) four span beam (EB3), (d) six span beam (EB4), (e) ten span beam (EB5) and (f) fifteen span beam (EB6)

Example beams have been chosen in such a way that most of the input parameters have not been considered in the training, validating or testing and none of the combinations of input parameters has been used in the training, validating or testing. The values of $d^i$ for the spans, obtained from the iterative analysis and the neural networks, along with the percentage errors are shown in Table 3. The values have been reported only for those spans, for which $d^e$ is not small. As indicated earlier, $d^i$ for more than three span beams have been predicted using networks developed for nine span beams (NN4- NN6). The maximum error in prediction of $d^i$ for any span of example beams is 5.11%. The root mean square

percentage error in prediction of inelastic mid-span deflections $d^i$ for the example beams is 2.22%. The percentage errors are therefore small for practical purposes. Also, the neural networks developed for nine span beam are found to be applicable for all beams having more than three spans.

Table 3. Actual and predicted inelastic midpsan deflections, $d^i$ for example beams

| Beam | Span No. | Elastic deflection (mm) | Inelastic deflection(mm) | | % Error |
|---|---|---|---|---|---|
| | | | Actual | Predicted | |
| EB1 | 01 | 12.252 | 14.5833 | 14.4837 | -0.6830 |
| | 02 | 4.8268 | 6.4246 | 6.3567 | -1.0569 |
| EB2 | 01 | 5.6011 | 6.7758 | 6.7756 | -0.0030 |
| | 02 | 24.116 | 30.2219 | 30.7707 | 1.8159 |
| | 03 | 1.8271 | 2.3842 | 2.4067 | 0.9437 |
| EB3 | 01 | 0.7541 | 0.7984 | 0.7630 | -4.4339 |
| | 02 | 5.3430 | 7.4483 | 7.2466 | -2.7075 |
| | 03 | 15.134 | 19.6674 | 19.4934 | -0.8847 |
| EB4 | 01 | 1.0393 | 1.4138 | 1.4525 | 2.7373 |
| | 02 | 8.1858 | 10.0792 | 9.9518 | -1.2640 |
| | 03 | 6.6230 | 9.0510 | 8.9496 | -1.1203 |
| | 04 | 7.9771 | 10.6132 | 10.4044 | -1.9674 |
| | 05 | 16.0681 | 23.6722 | 22.6329 | -4.3904 |
| | 06 | 29.8376 | 34.5995 | 36.3692 | 5.1148 |
| EB5 | 01 | 4.2734 | 4.4839 | 4.4338 | -1.1173 |
| | 03 | 2.2256 | 2.4781 | 2.4839 | 0.2341 |
| | 04 | 3.8077 | 4.6011 | 4.5844 | -0.3627 |
| | 05 | 1.1865 | 1.7164 | 1.6938 | -1.3167 |
| | 06 | 4.8850 | 5.6539 | 5.6443 | -0.1691 |
| | 08 | 0.5288 | 0.4698 | 0.4830 | 2.8097 |
| | 10 | 9.4754 | 10.2412 | 10.4161 | 1.7078 |
| EB6 | 01 | 2.8056 | 2.8510 | 2.8261 | -0.8737 |
| | 03 | 1.63104 | 1.6240 | 1.6094 | -0.8978 |
| | 04 | 1.64045 | 2.5184 | 2.5167 | -0.0683 |
| | 05 | 22.5459 | 29.3760 | 29.3880 | 0.0411 |
| | 06 | 1.78479 | 2.7201 | 2.5979 | -4.4947 |
| | 07 | 1.4820 | 1.6190 | 1.5711 | -2.9586 |
| | 08 | 0.5011 | 0.4857 | 0.4727 | -2.6846 |
| | 09 | 0.6318 | 0.9866 | 0.9798 | -0.6933 |
| | 10 | 10.4580 | 13.0503 | 13.0454 | -0.0372 |
| | 11 | 2.3552 | 4.0707 | 3.9879 | -2.0331 |
| | 12 | 11.2542 | 14.0098 | 13.9798 | -0.2145 |
| | 13 | 0.9885 | 1.20183 | 1.1561 | -3.8025 |
| | 15 | 9.0295 | 9.9188 | 9.7335 | -1.8682 |

## 8. CONCLUSION

1. In order to obtain the change in mid-span deflection of a span (say $j^{th}$) of a continuous composite beam with sufficient accuracy, cracking at the supports (supports $j$ and $j+1$) of the span and adjacent supports (supports $j-1$ and $j+2$) only needs to be considered.
2. The significant structural parameters that govern $\delta d_j / d_j^{eq}$ are identified to be $I^{cr}/I^{un}$, $S_{j-1}/S_j$, $S_{j+1}/S_j$, $w_{j-1}/w_j$, $w_{j+1}/w_j$, $M^{cr}/M^e_{j-1}$, $M^{cr}/M^e_j$, $M^{cr}/M^e_{j+1}$, $M^{cr}/M^e_{j+2}$. The parameter $\delta d/d^{eq}$ is independent of absolute span length.
3. Based on the methodology presented, six neural networks have been developed (Table 2) depending on number of spans in beams and position of spans in the beams. The neural networks developed for nine span beams are found to be applicable for all the beams having more than three spans.

4. The neural networks have been validated for a number of example beams with different number of spans. The root mean square in prediction of inelastic deflections is found to be 2.22%, which is small for practical purposes.

The application of the methodology presented herein to the composite beams is a step towards rapid estimation of inelastic deflections in large composite building frames where a very large computational effort is required in the iterative method. Further, the methodology can also be extended for the time-dependent analysis of composite beams and frames where a huge saving in computational effort would result.

## NOTATIONS

| | |
|---|---|
| $E$ | modulus of elasticity |
| $I$ | transformed moment of inertia of a section about its neutral axis |
| $I^{cr}/I^{un}$ | inertia ratio |
| $M$ | moment |
| $M^{cr}/M^{e}$ | cracking moment ratio |
| $S$ | stiffness |
| $S_{j-1}/S_j$ , $S_{j+1}/S_j$ | stiffness ratios |
| $d$ | mid-span deflection |
| $l$ | span length |
| $n$ | number of spans |
| $w$ | uniformly distributed load |
| $w_{j-1}/w_j$ , $w_{j+1}/w_j$ | load ratios |
| $\eta$ | variation in elastic moment with respect to $l$ |
| $\delta d$ | $d^i - d^e$ |

***Subscript***

| | |
|---|---|
| $j$ | support or span number |
| $c$ | concrete |

***Superscript***

| | |
|---|---|
| $e$ | elastic |
| $eq$ | equivalent |
| $cr$ | cracking |
| $i$ | inelastic |
| $un$ | uncracked |

***Acknowledgement*:** This work was supported by the Department of Science and Technology, Ministry of Science and Technology, Government of India (Project No. SR/S3/MERC/0023/2008). The authors express their gratitude for the support.

## REFERENCES

1. Ghali, A., Favre, R. & Elbadry, M. (2002). *Concrete structures: Stresses and deformations*. 3rd ed., Spon Press, London.
2. Kawamura, K., Miyamoto, A., Frangopol, D. M. & Abe, M. (2004). Performance evaluation system for main reinforced concrete girders of existing bridges. *Transportation Research Record,* Vol. 1866, pp. 67-78.
3. Feng, Q. M., Kim, D. K., Yi, J. H. & Chen, Y. (2004). Baseline models for bridge performance monitoring. *Journal of Engineering Mechanics*, ASCE, Vol. 130, No. 5, pp. 562-569.

4. Maru, S. & Nagpal, A. K. (2004). Neural network for creep and shrinkage deflections in reinforced concrete frames. *Journal of Computing in Civil Engineering*, ASCE, Vol. 18, No. 4, pp. 350-359.
5. Kim, J. I., Kim, D. K., Feng, M. Q. & Yazdani, F. (2004). Application of neural networks for estimation of concrete strength. *Journal of Materials in Civil Engineering*, ASCE, Vol. 16, No. 3, pp. 257-264.
6. Kim, D. K., Lee, J. J., Lee, J. H. & Chang, S. K. (2005). Application of probabilistic neural networks for prediction of concrete strength. *Journal of Materials in Civil Engineering*, ASCE, Vol. 17, No. 3, pp. 353-362.
7. Guzelbey, I. H., Cevik, A. & Erklig, A. (2006). Prediction of web crippling strength of cold-formed steel sheetings using neural networks. *Journal of Constructional Steel Research*, Vol. 62, pp. 962-973.
8. Chaudhary, S., Pendharkar, U. & Nagpal, A. K. (2007). Bending moment prediction for continuous composite beams by neural networks. *Advances in Structural Engineering*, Vol. 10, pp. 439-454.
9. Shahin, M. & Elchanakani, M. (2008). Neural networks for ultimate pure bending of steel circular tubes. *Journal of Constructional Steel Research*, Vol. 64, pp. 624-633.
10. Caglar, N. (2009). Neural network based approach for determining the shear strength of circular reinforced concrete columns. *Construction and Building Materials*, Vol. 23, pp. 3225-3232.
11. Arslan, M. H. (2010). Predicting of torsional strength of RC beams by using different artificial neural network algorithms and building codes. *Advances in Engineering Software*, Vol. 41, pp. 946-955.
12. Hodhod, H. & Abdeen, M. A. M. (2011). Simulation and prediction for the effect of natural and steel fibers on the performance of concrete using experimental analyses and artificial neural networks numerical modeling. *Journal of Civil Engineering*, KSCE, Vol. 15, No. 8, pp. 1373-1380.
13. Uddin, M. A., Jameel, M., Razak, H. A. & Islam, A. B. M. (2012). Response prediction of offshore floating structure using artificial neural network. *Advanced Science Letters*, Vol. 14, pp. 186-189.
14. Arya, F. K. & Ayati, B. (2013). Application of artificial neural networks for predicting COD removal efficiencies of rotating disks and packed-cage RBCs in treating hydroquinone. *Iranian Journal of Science and Technology, Transactions of Civil Engineering*, Vol. 37, No. C2, pp. 325-336.
15. Rakhshandehroo, G. R. & Ghadampour, Z. (2011). A combination of fractal analysis and artificial neural network to forecast groundwater depth. *Iranian Journal of Science and Technology, Transactions of Civil and Environmental Engineering*, Vol. 35, No. C1, pp. 121-130.
16. Ghaffarzadeh, H. (2013). Response spectrum based generation of spatially varying earthquake using artificial neural networks. *Iranian Journal of Science and Technology, Transactions of Civil Engineering*, Vol. 37, No. C2, pp. 233-242.
17. Noruzi, K. & Rakhshandehroo, G. R. (2007). Most probable pollution source identification in rivers by neural networks. *Iranian Journal of Science and Technology, Transaction B, Engineering*, Vol. 31, No. B5, pp. 501-508.
18. Mohammadhassani, M., Nezamabadi-Pour, H., Jumaat, M. Z., Jameel, M. & Arumugam, A. M. S. (2013). Application of artificial neural networks (ANNs) and linear regressions (LR) to predict the deflection of concrete deep beams. *Computers and Concrete*, Vol. 11, No. 3, pp. 237-252.
19. Mohammadhassani, M., Nezamabadi-Pour, H., Jumaat, M. Z., Jameel, M., Hakim, S. J. S. & Zargar, M. (2013). Application of the ANFIS model in deflection prediction of concrete deep beam. *Structural Engineering and Mechanics*, Vol. 45, No. 3, pp. 319-332.
20. Chaudhary, S., Pendharkar, U. & Nagpal, A. K. (2007). An analytical-numerical procedure for cracking and time-dependent effects in continuous composite beams under service load. *Steel and Composite Structures*, Vol. 7, No. 3, pp. 219-240.
21. Chaudhary, S., Pendharkar, U. & Nagpal, A. K. (2007). Hybrid procedure for cracking and time-dependent effects in composite frames at service load. *Journal of Structural Engineering*, ASCE, Vol. 133, No. 2, pp. 166-175.

22. Comite´ Euro International du Beton-Fe´de´ration International de la Pre´contrainte, (CEB-FIP). (1993). *Model code for concrete structures.* Thomas Telford, London.
23. Hsu, D. S., Yeh, I. C. & Lian, W. T. (1993). Artificial neural damage detection of existing structure. *Proc 3rd ROC and Japan Seminar on Natural Hazards Mitigation*, Tainan, pp. 423-436.
24. Sttutgart Neural Network Simulator (SNNS) user manual. Version 4.2. University of Sttutgart: Institute for Parallel and Distributed High Performance Systems (IPVR), http://www-ra.informatik.uni-tuebingen.de/SNNS/ (December 27, 2012).
25. Reich, Y. & Barai, S. V. (1999). Evaluating machine learning models for engineering problems. *Artificial Intelligence in Engineering*, Vol. 13, pp. 257-272.